Micro and Nanostructures 185 (2024) 207708

Contents lists available at ScienceDirect

Micro and Nanostructures

journal homepage: www.journals.elsevier.com/micro-and-nanostructures

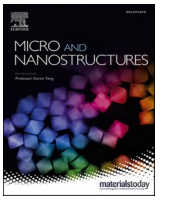

Nanostructures of boron nitride: A promising nanocarrier for anti-cancer drug delivery

Saade Abdalkareem Jasim [a,b], Mohammed Sabar Al-Lami [c,d], Ameer A. J [e], A.H. Shather [f], Ahmed Khalid Aldhalmi [g], Anmar Ghanim Taki [h], Batool Ali Ahmed [i], Mais Mazin Al-Hamdani [j], Shelesh Krishna Saraswat [k,*]

[a] *Pharmacy Department, Al-huda University College, Anbar, Iraq*
[b] *Biotechnology Department, College of Applied Science, Fallujah University, Anbar, Iraq*
[c] *College of Pharmacy, University of Basrah, Basrah, Iraq*
[d] *College of Pharmacy, National University of Science and Technology, Thi Qar, Iraq*
[e] *Al-Zahraa University for Women, Karbala, Iraq*
[f] *Department of Computer Engineering Technology, Al Kitab University, Altun Kopru, Kirkuk, 00964, Iraq*
[g] *College of Pharmacy, Al- Mustaqbal University, 51001, Hilla, Babylon, Iraq*
[h] *Department of Radiology & Sonar Techniques, Al-Noor University College, Nineveh, Iraq*
[i] *Department of Medical Engineering, Al-Nisour University College, Baghdad, Iraq*
[j] *College of Pharmacy, Al-Ayen University, Thi-Qar, Iraq*
[k] *Reserch Center, GlA University, Mathura 281406, India*

ARTICLE INFO

Keywords:
Hydroxyurea molecule
Adhesion energy
Drug delivery
Gaseous phase

ABSTRACT

Within this study, we investigate the interaction of the hydroxyurea molecule with a boron nitride nanocone (BNC), a boron nitride nanosheet (BNS), and a boron nitride nanotube (BNT) as nanostructures for the purpose of drug delivery by performing DFT computations. DFT computations on the models under study are performed by considering gas and water phases. Based on the adhesion energy values, we obtain a stabilized complex of hydroxyurea and BNC, BNS and BNT in the gas and water phases. The negative values of adhesion energy demonstrate that the reaction is exothermic. Based on the results of the QTAIM, the electron density values in the bond critical points are positive and low in all hydroxyurea-bonding complexes. Based on the calculational results, there are weak interaction forces for the significant and efficient release of hydroxyurea from the carriers at target sites. The impact of molecular adhesion upon the electronic attributes of BNC, BNS and BNT is examined by investigating the density of states, and based on the results, BNC is nearer to the Fermi energy compared to BNS and BNT. The adhesion energy values are higher in the gaseous phase compared to the water phase, which indicates that the interaction of the molecule with BNC, BNS and BNT is stronger in the gaseous phase. The interaction of hydroxyurea with BN stronger than its interaction with BNS and BNT based on the adhesion energy values. Following the adhesion of hydroxyurea, ΔE_g was – 1.56 eV, −0.16 eV, and −0.12 eV for BNC, BNS, and BNT, respectively, which showed the higher sensitivity of BNC compared to BNS and BNT. Based on the computations, BNC, BNS, and BNT can be used as a promising carrier for hydroxyurea.

* Corresponding author.
E-mail address: sheleshkrishnasaraswat@gmail.com (S. Krishna Saraswat).

https://doi.org/10.1016/j.micrna.2023.207708
Received 23 September 2023; Received in revised form 5 November 2023; Accepted 6 November 2023
Available online 8 November 2023

1. Introduction

There has been a rise in the number of disorders and diseases due to the dominant role of industrial and technological productions, which have affected the environment, human life and other living systems negatively [1,2]. In spite of the improvement in medical protocols, there is a lack of protocols for treating serious diseases like cancer and viral pandemics [3,4]. As a result, one of the hot topics is the development and design of new drugs and their optimization [5–9]. Numerous research studies have been carried out into synthesizing and characterizing new pharmaceutical compounds [10–13]. In particular, many studies have been carried on drugs studies in order to develop new attributes for drug delivery systems (DDSs), particularly following the discovery of nano-structures [14,15]. After their discovery, researchers investigated the potential use of carbon nanostructures in biological systems and for drug delivery [16]. Developing nanomaterial-based DDSs can be conducive to increasing the efficiency and bioavailability of antiviral drugs. Unlike conventional methods, using nano-materials in drug delivery has many advantages, including increased drug reaction time, enhanced bioavailability, reduced side effects, and sustained drug release [17].

Research have investigated the potential applications of different nanocarbons (e.g., fullerenes, carbon nanotubes and graphene derivatives) in bioimaging, cell targeting and drug delivery [18–23]. Nevertheless, it is necessary to investigate their toxicity [24–28]. The chemical stability of boron nitride nano-materials is higher than the chemical stability of carbon nano-materials, which makes them suitable for biomedical purposes [29]. As an example, based on recently performed studies, biocompatibility and cytotoxicity of boron nitride nanotubes are higher than biocompatibility and cytotoxicity of carbon nanotubes [30–34]. In the past years, some researchers have been reported the ability of different 2D materials for smart drug delivery [35–39]. for example, the graphdiyne nanosheet can be used for sorafenib and regorafenib drugs delivery as theoretical approaches [40]. Also, the boron nitride nanosheet was used as a nanocarrier for different anti-cancer drugs such as 5-fluorouracil (FU), 6-mercaptopurine (MP) and 6-thioguanine (TG) [41–43]. In addition, the 2D phosphorene was introduced a novel nanocarrier for anti-cancer drugs delivery systems [44]. Yet, more research should be done into boron nitride nanomaterials to confirm their application in biological systems. Due to its high chemical stability, oxidation resistance, large surface area, high thermal stability, mechanical strength and high thermal conductivity, researchers have focused on hexagonal BN sheets, which are similar to graphite carbon nitride (g-C_3N_4) and graphene [45–47]. (BNNTs), which are structurally analogous to carbon nanotubes, have introduced a biocompatible nanoplatform for drug delivery. Researchers have suggested the application of BNNTs have been in nanocomposites for developing new piezoelectric and functional materials because of their chemical stability and unique electrical and mechanical attributes. The biocompatibility of BNNTs is higher than that of carbon nanotubes. Also, they are considered nontoxic based on the data available in the literature [48–52]. In recent years, the focus has turned to carbon fullerenes and nanotubes with curved nanoscale structures owing to their mechanical and electronic attributes [53]. Inserting topological defects and pentagonal atomic rings into the hexagonal network of CNTs might result in the closure of the tubes and an increase in the local curvature [54]. The cap structure is dependent upon the special defect included, but it is generally has a similar conical surface with electronic attributes different to those of bulk materials [55]. This is also the case for BN nano-cones. They could be formed either as free-standing structures or as closing caps at the edges of BNNTs [55]. As a result, different BN nano-structures are considered conducive to giving new properties to nano-structures. Within this work, various compounds such as BNNTs, BNNCs, and BNNSs were examined for their potential application in the drug delivery of hydroxyurea.

Hydroxyurea, also known as Hydrea, is one of the anti-cancer medications used for treating different cancer types such as carcinoma, leukemia and melanoma [56]. It is capable of inhibiting the growth of cancerous in the body, thus limiting the increase in the cancer [57]. Nonetheless, there are common side effect associated with hydroxyurea such as bleeding and decreased blood cells [58]. There are many studies into improving the efficiency of hydroxyurea, but the evidence is not conclusive [59]. SO, more research studies must be done on hydroxyurea to increase its efficiency and minimize its side effects. It is worth mentioning that one of the most crucial issues in research on living systems is the topic of human health care systems [6,60,61]. Hence, we investigated the possible use of BNNTs, BNNCs, and BNNSs as viable DDSs for hydroxyurea by examining the adhesion of hydroxyurea on these nano-structures. Here, the selective loading of hydroxyurea was done on BNNTs, BNNCs, and BNNSs. NBO computations were undertaken for these model systems to characterize the charge transports and interactions between hydroxyurea and with the above-mentioned nano--structures. DFT computations were undertaken for assessing the possible use of these nano-structures as a carrier for hydroxyurea.

2. Computational details

Here, we scrutinized the possibility of using carbon nano-structures in the drug delivery of hydroxyurea. Using the basis set the 6–31 G (d) and M06-2X method, we undertook DFT computations via GAMESS-US software [62,63]. In the present study, Grimme's semi-empirical correction was used interaction energies, which accurately describes dispersion forces which are considered important in investigating adhesion processes. We aimed at obtaining the results related to the NBO analysis, molecular-electronic potential (MEP) levels and density of states (DOSs) [64,65]. The adhesion energy of hydroxyurea molecule on the nano-structures' surface can be computed using the below equation [66]:

$$E_{ads} = \left(E_{complex}\right) - \left(E_{nanostructure} + E_{Hyd}\right) \quad (1)$$

where, $E_{complex}$, $E_{Hydroxyurea}$ and $E_{nanostructure}$, respectively, are the total energies of nano-structures@hydroxyurea, individual hydroxyurea molecule and nanostructures. A negative adhesion energy shows that the adhesion process is exothermic. The self-consistence field convergence criterion has been set to 10^{-6}. Also, for optimizations, the maximum displacement, that is, the maximum structural change of one coordinate as well as the average (RMS) change over all structural parameter thresholds were set

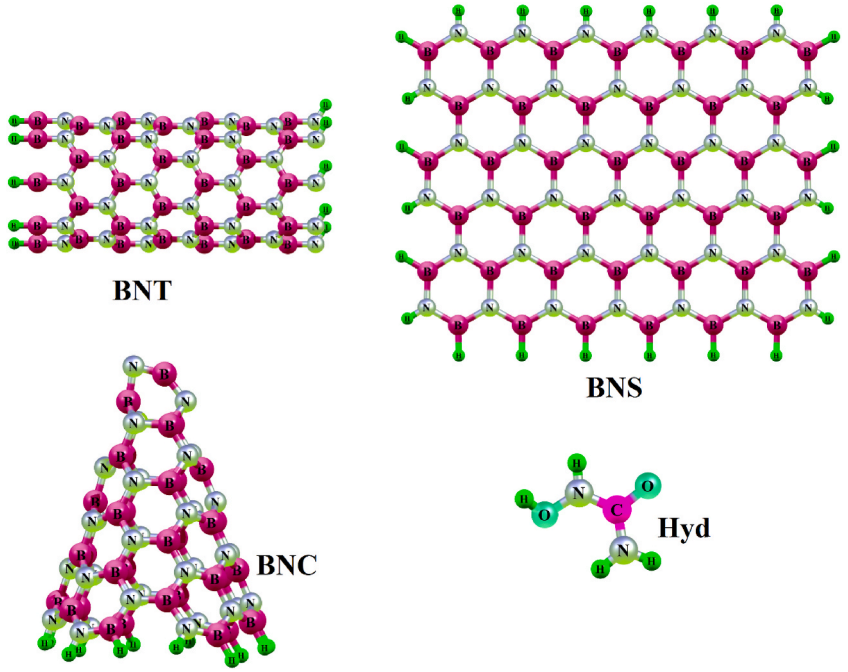

Fig. 1. Optimized structures of BNT, BNS, BNC, and Hydroxyurea drug.

Table 1
Adhesion energy (E_{ads}) of Hydroxyurea molecule on the nano-structures in two phases of gas and water, transferred charge between the molecule and nano-structures (Q_T), HOMO-LUMO energy gaps (E_g), and change in HOMO-LUMO gap of different BN nano-structures upon the adhesion process.

Sample	$E_{ads\text{-}gas}$ (eV)	$E_{ads\text{-}water}$ (eV)	E_g (eV)	ΔE_g	Q_T (e)
BNT	–	–	3.27	–	–
BNS	–	–	4.51	–	–
BNC	–	–	4.63	–	–
BNT@Hydroxyurea	−0.094	−0.047	3.15	0.12	0.046
BNS@Hydroxyurea	−0.102	−0.065	4.35	0.16	0.049
BNC@Hydroxyurea	−0.137	−0.084	3.07	1.56	0.089

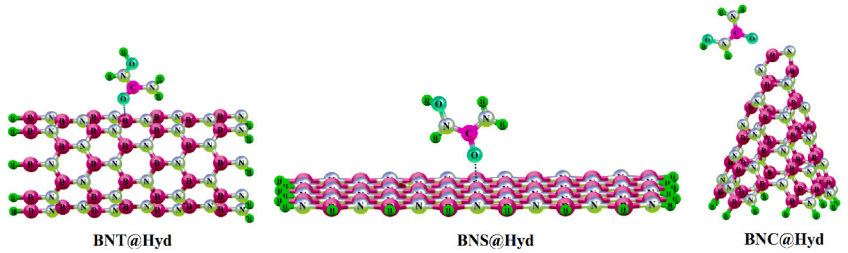

Fig. 2. Optimized structures of different BN nano-structures with Hydroxyurea drug.

about 1.8×10^{-4} and 1.2×10^{-4}, respectively. The maximum remaining force on an atom in the system as well as the average root mean square (RMS) force on all atoms thresholds were set to be about 4.5×10^{-4} and 3.0×10^{-4}, respectively.

3. Results and discussion

3.1. Hydroxyurea drug adhesion onto BNT, BNC, and BNS

The optimized structure of BNT and the hydroxyurea is shown in Fig. 1. The model of BNT with 56 B, 56 N, and 16H atoms was an (8,0) zigzag nano-tube with a length and diameter of 14 Å and 6.5 Å respectively. In addition to the tubular structure, we could identify

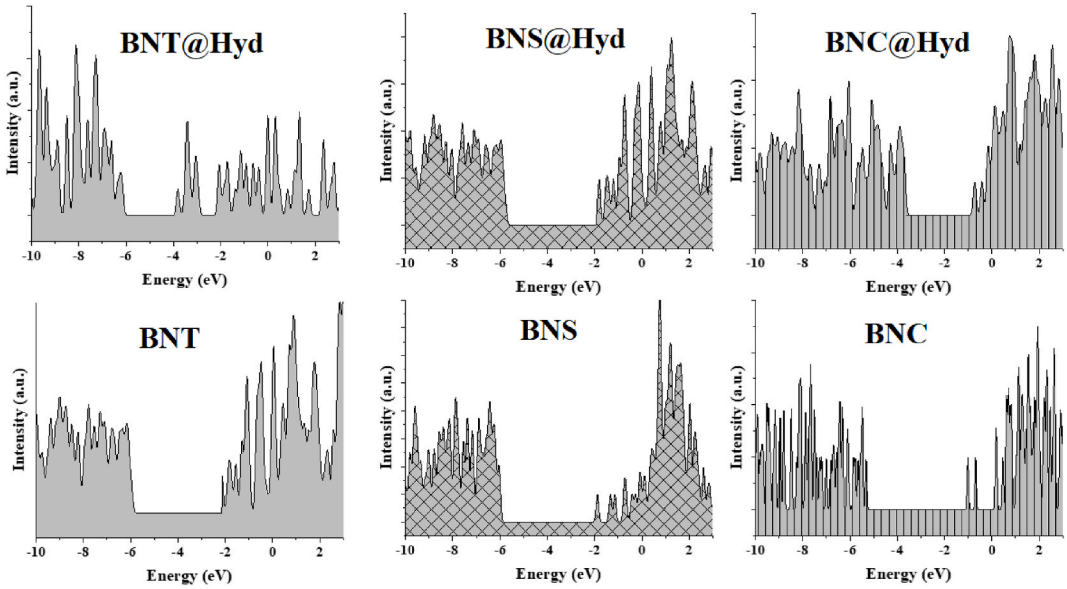

Fig. 3. The DOS plot of different BN nano-structures with Hydroxyurea drug.

2 B–N bonds and lengths. One was associated with the nanotube axis and its length was 1.41 Å, and another was diagonal and its length was 1.44 Å. The dangling B–N bonds were saturate for the sake of avoiding dangling effects in BNT, which was of high necessity because of the lack periodic boundary conditions in the molecular computations. The computed energy gap of 3.27 eV is listed in Table 1. Initially, hydroxyurea had an adhesion onto different sites onto the exterior NT surface with various orientations. The most stable site of Hydroxyurea on the surface of BNT was obtained following the optimization and distance between them was computed (Fig. 2). There was a change in the adhesion energy, transported charge, energy and band gaps values with pre-adhesion ΔE_g of hydroxyurea. The charge transfer values computed by the NBO analysis was 0.046 (e), which indicated charge transport was from hydroxyurea to BNT. The energy gap was 3.15 eV, which changed slightly in comparison with that of BNT (3.27 eV). The reduction in the energy gap value indicated that there was an increase of conductance. The computed adhesion energy in the gaseous phase was - 0.094 eV, whereas it was - 0.047 eV in the water phase, showing the formation of a stronger bong by hydroxyurea with BNT in the gaseous phase. The reaction of hydroxyurea with BNT was exothermic because the adhesion energies were negative. These adhesion energies showed the noncovalent nature of interaction between BNT and hydroxyurea, which led to a physisorption. Hence, BNT cannot be used as the carrier of the hydroxyurea molecule.

To investigate the structural and electronic attributes of BNS, its structure was examined with and without the hydroxyurea molecule. According to the optimized geometry of BNS shown in Fig. 1, there is a B–N bond between the hexagons and its length is 1.43 Å. The energy gap of BNS was 4.51 eV. The adhered molecule was initially located at various sites onto BNS with various orientations for finding the most stable configuration for surface adhesion. The most stable site of hydroxyurea onto BNS was obtained following the optimization, (see Fig. 2). As illustrated in Table 1, the adhesion energies in the gaseous and water phases were - 0.102 eV and - 0.065 eV respectively. This demonstrates that a stronger bond was formed by the gaseous phase. Based on the negative adhesion energies, the reaction was exothermic. The value of 4.35 eV for BNS@ hydroxyurea and the electron-donating rate of the molecule at BNS that was 0.049 (e) demonstrate that there is a slight reduction in the energy gap in comparison with value computed for BNS. The adhesion energy value demonstrated the physisorption of hydroxyurea on BNS through a noncovalent interaction, confirming the possibility of using BNS as a carrier of hydroxyurea. Furthermore, the obtained ΔE_g value for BNS@ hydroxyurea was higher compared to that of BNT@ hydroxyurea. This shows that it was more conductive than BNT@ hydroxyurea.

Fig. 1 shows the most stable geometry of BNC. The length and the angle of the bond located on the top of BNC was different from the rest. The angles of B–N–B and N–B–N bonds on the top of BNC were approximately 104–109°, whereas the bond angles of at the bottom increased to 118–120° for B–N–B and N–B–N, respectively. The different orbital hybridization of N atoms at the top and bottom of BNC is the reason for this dramatic variation in the bond angles. The hybridization had similarity to sp^3 for N atoms on the top layer of BNC, whereas it had similarity to sp^2 for N atoms at the bottom. However, the hybridization of B atoms was similar to sp^2 at the top and bottom layers. The length of the B–N bond was around 1.44–1.45 Å for layers which located in the middle. The energy gap of BNC was around 4.63 eV. The Hydroxyurea molecule was structurally optimized to investigate the structural and electronic attributes of BNC. The molecule was initially located at various sites on the exterior surface of BNC with different orientations to find the most stable adhesion site, which was shown in Fig. 2 following the optimization. The distance between the BNC and hydroxyurea is also shown in Fig. 2. Based on the low adhesion energies obtained for BNC@Hydroxyurea in the gaseous and water phases (-0.137 eV, - 0.84 eV), hydroxyurea was physiosorbed through a noncovalent interaction. Also, based on the adhesion energies, the binding between hydroxyurea and BNC was stronger in the gaseous phase. Moreover, the adhesion energies were negative, which indicated that the reaction between hydroxyurea and BNC was exothermic. The value of Q_T was −0.089 (e), showing the electron-accepting nature of

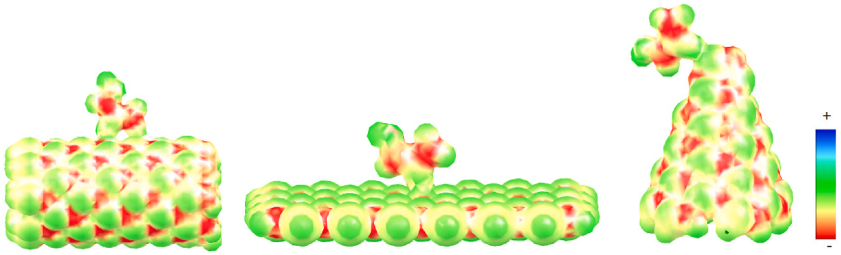

Fig. 4. Calculated molecular electrostatic potential (MEP) surfaces of different BN nano-structures with Hydroxyurea drug.

hydroxyurea in the BNC@Hydroxyurea structure. In spite the fact that adhesion energy was greater than that of BNT@Hydroxyurea and BNS@Hydroxyurea, it was also regarded as a physisorption. The value of energy gap after adhesion (3.07 eV) in Table 1 demonstrated that there was dramatic change in comparison with the energy gap of BNS and BNT after adhesion. Following the adhesion of the molecule (ΔE_g = - 1.56 eV), there was a decrease in the energy gap, showing a dramatic conductance for BNC following the adhesion of hydroxyurea. Hence, we can consider BNC a sensor for hydroxyurea.

3.2. DOS analysis

To examine the impact of surface adhesion of the hydroxyurea on the electronic attributes of nano-structures, the DOS analysis was performed. The results were provided in Fig. 3. The proximity of BNC the Fermi energy level was more than BNS and BNT. As shown in the DOS plots, the surface adhesion of the molecule on BNC had an impact on it and the energy level of BNT and BNS remained constant following the adhesion of hydroxyurea. The ΔE_g for the adhesion of hydroxyurea on BNC, BNS and BNT were – 1.56 eV, - 0.16 eV and - 0.12 eV, respectively, under optimal conditions. These values indicated that there was a weaker interaction between Hydroxyurea and BNC than BNS and BNT. The DOS analysis revealed that there was a significant change in the Fermi level changes for BNC. However, the physisorption of hydroxyurea took place on the BNC surface. So, the system had more conductance. Based on Eq. (2), a dramatic change is expected in the conductance of the cluster due to the adhesion [67]:

$$\sigma \propto \exp\left(-\frac{E_g}{2kT}\right) \tag{2}$$

where K and σ are the Boltzmann constant and conductance respectively. Based on Eq. (2), if the energy gap becomes lower at a certain temperature, the conductance will be higher. Nevertheless, the energy gap of BNC@Hydroxyurea was significantly more than the energy gap of BNC. As conductance is proportionally related to the reduction of energy gap, we can assume that conductance increases with a reduction in the energy gap. The electrical attributes of BNC towards the surface adhesion of hydroxyurea were evidenced by this great sensitiveness. As BNC converted the presence of a hydroxyurea molecule directly into an electrical signal, we can use it to detect the hydroxyurea molecule. However, hydroxyurea did not impact on the electrical attributes of BNT and BNS. Hence, we could infer that BNC could selectively detect the hydroxyurea molecule.

3.3. MEP surfaces analysis

In order to provide an explanation for the load distributions by assessing the interaction between hydroxyurea and the nano-structures in different volumes, the MEP surface analysis was performed. The MEP surface analysis generated by the molecular charge distributions can be computed as follows [68]:

$$V(r) = \sum_A \frac{Z_A}{|R_A - r|} - \int \frac{\rho(r')dr'}{|r - r'|}$$

where Z_A signifies the nucleus charge at RA. The dominance of electrons or nuclei at a certain point determined V (r) sign. The MEP analysis in Fig. 4 shows that the atoms are both positively and negatively charge, donated by blue and red colors respectively. According to the MEP, the interaction between hydroxyurea and BNC can lead to a charge transport from BNC to the hydroxyurea molecule, which can further lead to van der Waals bonding at the surface. Also, the adhesion of hydroxyurea on CNS and BNT resulted in a charge transport from hydroxyurea to BNS and BNT.

3.4. QTAIM analysis

One of the widely used theories for gaining an understanding of interaction and analyzing electron density distributions is the quantum theory of atoms in molecules (QTAIM). QTAIM was developed from concepts from physics and quantum mechanics. QTAIM adopts a topological approach for localizing atoms in molecules in modeling a chemical bonding. Different types of interactions and bonds can be identified through a set of accessible points named bond critical points (BCPs). The maximum or minimum electron

Table 2
Topological parameters (au) at BCP of interaction of different BN nano-structures upon the adhesion process.

Sample	BCP	ρ_x	$\nabla^2\rho$	H
BNT@Hydroxyurea	H–N	0.00291	0.0062	0.00031
	O–B	0.0043	0.0166	0.00059
BNS@Hydroxyurea	H–N	0.0076	0.0306	0.0006
	O–B	0.0052	0.0347	0.0019
BNC@Hydroxyurea	H–N	0.0123	0.0359	0.0008
	O–B	0.0086	0.0437	0.0023

density is dependent upon the motion in both directions at BCPs. In general, QTAIM is one of the techniques adopted for investigating and assessing the significant attributes of bonds.

Hence, we adopted the QTAIM theory for investigating attributes of BCPs in hydroxyurea in the complex systems. To determine the nature of the interactions, after placing BCPs, we extracted the charge density (ρ_r) and its Laplacian ($\nabla^2\rho$). The electron energy density at BCPs is commonly applied for describing their energetic attributes (H). Based on the QTAIM computations, the electron density values at BCPs (ρ_r) were positive and low in all hydroxyurea bonding complexes, which is why van der Waals are formed (see Table 2). The electron density value BCPs shows that bonding is weak. Electrostatic interactions and charge transport are the main reason for the stability energy of these complexes, which might act in the same directions in some situations and in the opposite directions in other situations. Also, the bonding type in this interaction is dependent upon the electron density at BCPs. A positive $\nabla^2\rho$ and H at BCPs demonstrates that the density is low. Therefore, it is a van der Waals bond due to the weak interactions.

4. Conclusion

The present work aimed at investigating the possible application of BNC, BNT, and BNS for drug delivery by examining their interaction with Hydroxyurea through DFT computations. Based on the results, loading hydroxyurea on these nano-structures was possible. Also, based on the FMO analyses, there were dramatic changes in the models for the adhered hydroxyurea molecule on BNC. The energy gap values indicated a stronger interaction between Hydroxyurea and BNC compared to other nano-structures. The ΔEg value for BNC following the adhesion of hydroxyurea was – 1.56 eV, which showed an increase in the conductance of the nano-carrier following the adhesion of hydroxyurea. Hence, BNC can be proposed a suitable vehicle for hydroxyurea. The MEP analysis demonstrated that the atoms are both negatively and positively (red color and blue color) charged. Based on the QTAIM computations, the interactions between Hydroxyurea and the nano-structures were weak. So, BNC, BNT, and BNS can be used as suitable carriers for hydroxyurea.

Declaration of competing interest

The authors declare that they have no known competing financial interests or personal relationships that could have appeared to influence the work reported in this paper.

Data availability

No data was used for the research described in the article.

References

[1] A.T. Jalil, S.H. Dilfy, A. Karevskiy, N. Najah, Viral hepatitis in Dhi-Qar Province: demographics and hematological characteristics of patients, Int. J. Pharmaceut. Res. 12 (2020) 2081–2087.
[2] G. Widjaja, A.T. Jalil, H.S. Rahman, W.K. Abdelbasset, D.O. Bokov, W. Suksatan, M. Ghaebi, F. Marofi, J.G. Navashenaq, F. Jadidi-Niaragh, Humoral immune mechanisms involved in protective and pathological immunity during COVID-19, Hum. Immunol. 82 (2021) 733–745.
[3] P.A. Ghamsari, M. Samadizadeh, M. Mirzaei, Halogenated derivatives of cytidine: structural analysis and binding affinity, J. Theor. Comput. Chem. 19 (2020), 2050033.
[4] A.T.J. Marwan Mahmood Saleh, R.A. Abdulkareem, A.A. Suleiman, Evaluation of Immunoglobulins, CD4/CD8 T Lymphocyte Ratio and Interleukin-6 in COVID-19 Patients, 2020.
[5] F. Marofi, O.F. Abdul-Rasheed, H.S. Rahman, H.S. Budi, A.T. Jalil, A.V. Yumashev, A. Hassanzadeh, M. Yazdanifar, R. Motavalli, M.S. Chartrand, CAR-NK cell in cancer immunotherapy; A promising frontier, Cancer Sci. 112 (2021) 3427–3436.
[6] M.M. Kadhim, N. Sheibanian, D. Ashoori, M. Sadri, B. Tavakoli-Far, R. Khadivi, R. Akhavan-Sigari, The drug delivery of hydrea anticancer by a nanocone-oxide: computational assessments, Comput. Theor. Chem. 1215 (2022), 113843.
[7] S. Vakili-Samiani, A.T. Jalil, W.K. Abdelbasset, A.V. Yumashev, V. Karpisheh, P. Jalali, S. Adibfar, M. Ahmadi, A.A.H. Feizi, F. Jadidi-Niaragh, Targeting Wee1 kinase as a therapeutic approach in hematological malignancies, DNA Repair 107 (2021), 103203.
[8] Z.D. Alhattab, A.M. Aljeboree, M.A. Jawad, F.S. Sheri, A.K. Obaid Aldulaim, A.F. Alkaim, Highly adsorption of alginate/bentonite impregnated TiO2 beads for wastewater treatment: optimization, kinetics, and regeneration studies, Caspian J. Environ. Sci. 21 (2023) 657–664.
[9] A. Aljeboree, S. Essa, Z. Kadam, F. Dawood, D. Falah, A. Af, Environmentally friendly activated carbon derived from palm leaf for the removal of toxic reactive green dye, Int. J. Pharmaceut. Qual. Assur. 14 (2023) 12–15.
[10] V. Adole, Synthesis, antibacterial, antifungal and DFT studies on structural, electronic and chemical reactivity of (E)-7-((1H-Indol-3-yl) methylene)-1, 2, 6, 7-tetrahydro-8H-indeno [5, 4-b] furan-8-one, Adv. J. Chem.-Section A 4 (2021) 175–187.
[11] O. Raouf, S. Selim, H. Mohamed, O. Abdel-Gawad, A. Elzanaty, S. Abdel-Kader, Synthesis, characterization and biological activity of Schiff bases based on chitosan and acetophenone derivatives, AJCA 3 (2020) 274–282.

[12] M. Abosaooda, J.M. Wajdy, E. Hussein, A. Jalil, M. Kadhim, M. Abdullah, A. Hamed, H. Almashhadani, Role of vitamin C in the protection of the gum and implants in the human body: theoretical and experimental studies, Int. J. Corrosion and Scale Inhibition 10 (2021) 1213–1229.
[13] A.M. Aljeboree, Z.D. Alhattab, U.S. Altimari, A.K.O. Aldulaim, A.K. Mahdi, A.F. Alkaim, Enhanced removal of amoxicillin and chlorophenol as a model of wastewater pollutants using hydrogel nanocomposite: optimization, thermodynamic, and isotherm studies, Caspian J. Environ. Sci. 21 (2023) 411–422.
[14] A.T. Jalil, S. Ashfaq, D.O. Bokov, A.M. Alanazi, K. Hachem, W. Suksatan, M. Sillanpää, High-sensitivity biosensor based on glass resonance PhC cavities for detection of blood component and glucose concentration in human urine, Coatings 11 (2021) 1555.
[15] A.R. Oladipupo, C.S. Alaribe, T.A. Akintemi, H. Coker, Effect of Phaulopsis falcisepala (Acanthaceae) leaves and stems on mitotic arrest and induction of chromosomal changes in meristematic cells of Allium cepa, Prog Chem Biochem Res 4 (2021) 134–147.
[16] Y. Sun, X. Ma, H. Hu, Marine polysaccharides as a versatile biomass for the construction of nano drug delivery systems, Mar. Drugs 19 (2021) 345.
[17] V. Pilkington, T. Pepperrell, A. Hill, A review of the safety of favipiravir–a potential treatment in the COVID-19 pandemic? J. Vrus Erad. 6 (2020) 45–51.
[18] Z. Liu, W. Cai, L. He, N. Nakayama, K. Chen, X. Sun, X. Chen, H. Dai, In vivo biodistribution and highly efficient tumour targeting of carbon nanotubes in mice, Nat. Nanotechnol. 2 (2007) 47–52.
[19] Z. Liu, S. Tabakman, K. Welsher, H. Dai, Carbon nanotubes in biology and medicine: in vitro and in vivo detection, imaging and drug delivery, Nano Res. 2 (2009) 85–120.
[20] L. Zhang, J. Xia, Q. Zhao, L. Liu, Z. Zhang, Functional graphene oxide as a nanocarrier for controlled loading and targeted delivery of mixed anticancer drugs, Small 6 (2010) 537–544.
[21] D.A. Heller, S. Baik, T.E. Eurell, M.S. Strano, Single-walled carbon nanotube spectroscopy in live cells: towards long-term labels and optical sensors, Adv. Mater. 17 (2005) 2793–2799.
[22] X. Sun, Z. Liu, K. Welsher, J.T. Robinson, A. Goodwin, S. Zaric, H. Dai, Nano-graphene oxide for cellular imaging and drug delivery, Nano Res. 1 (2008) 203–212.
[23] A. Aljeboree, U. Altimari, M. Azeez, A. Alkaim, Spectrophotometric method for the determination of catechol amines drugs in pharmaceutical preparations, Int J Drug Deliv Technol 13 (2023) 213–216.
[24] J. Shi, H. Zhang, L. Wang, L. Li, H. Wang, Z. Wang, Z. Li, C. Chen, L. Hou, C. Zhang, PEI-derivatized fullerene drug delivery using folate as a homing device targeting to tumor, Biomaterials 34 (2013) 251–261.
[25] N. Lewinski, V. Colvin, R. Drezek, Cytotoxicity of nanoparticles, Small 4 (2008) 26–49.
[26] A.M. Pinto, I.C. Goncalves, F.D. Magalhaes, Graphene-based materials biocompatibility: a review, Colloids Surf. B Biointerfaces 111 (2013) 188–202.
[27] Z.H. Mahmoud, O.G. Hammoudi, A.N. Abd, Y.M. Ahmed, U.S. Altimari, A.H. Dawood, R. Shaker, Functionalize cobalt ferrite and ferric oxide by nitrogen organic compound with high supercapacitor performance, Results Chem. 5 (2023), 100936.
[28] H.A. Ghabbour, A.M. Fahim, M.A. Abu El-Enin, S.T. Al-Rashood, H.A. Abdel-Aziz, Crystal structure, Hirshfeld surface analysis and computational study of three 2-(4-arylthiazol-2-yl) isoindoline-1, 3-dione derivatives, Mol. Cryst. Liq. Cryst. 742 (2022) 40–55.
[29] A. Merlo, V. Mokkapati, S. Pandit, I. Mijakovic, Boron nitride nanomaterials: biocompatibility and bio-applications, Biomater. Sci. 6 (2018) 2298–2311.
[30] X. Chen, P. Wu, M. Rousseas, D. Okawa, Z. Gartner, A. Zettl, C.R. Bertozzi, Boron nitride nanotubes are noncytotoxic and can be functionalized for interaction with proteins and cells, J. Am. Chem. Soc. 131 (2009) 890–891.
[31] L. Li, L.H. Li, S. Ramakrishnan, X.J. Dai, K. Nicholas, Y. Chen, Z. Chen, X. Liu, Controlling wettability of boron nitride nanotube films and improved cell proliferation, J. Phys. Chem. C 116 (2012) 18334–18339.
[32] G. Ciofani, S. Danti, G.G. Genchi, B. Mazzolai, V. Mattoli, Boron nitride nanotubes: biocompatibility and potential spill-over in nanomedicine, Small 9 (2013) 1672–1685.
[33] M.A. Obaid, K.H. Harbi, A.N. Abd, Study the effect of antibacterial on the chemically prepared copper oxide, Mater. Today: Proc. 47 (2021) 6006–6010.
[34] S.A. Fadaam, H.M. Ali, A.A. Salih, M.A. Obaid, A.S. Ali, N.F. Habubi, Synthesis and characterization of metastable phases of SnO and Sn3O4 thin films for solar cells applications, in: Journal of Physics: Conference Series, IOP Publishing, 2021, 012003.
[35] A.M. Avachat, S.B. Bhise, Tailored release drug delivery system for rifampicin and isoniazid for enhanced bioavailability of rifampicin, Pharmaceut. Dev. Technol. 16 (2011) 127–136.
[36] R. Pandey, G. Khuller, Oral nanoparticle-based antituberculosis drug delivery to the brain in an experimental model, J. Antimicrob. Chemother. 57 (2006) 1146–1152.
[37] X. Pang, K. Gong, X. Zhang, S. Wu, Y. Cui, B.-Z. Qian, Osteopontin as a multifaceted driver of bone metastasis and drug resistance, Pharmacol. Res. 144 (2019) 235–244.
[38] L. Zhang, J. Zheng, S. Tian, H. Zhang, X. Guan, S. Zhu, X. Zhang, Y. Bai, P. Xu, J. Zhang, Effects of Al3+ on the microstructure and bioflocculation of anoxic sludge, J. Environ. Sci. 91 (2020) 212–221.
[39] A. Hota, S.G.K. Patro, A.J. Obaid, S. Khatak, R. Kumar, Constructed wetland challenges for the treatment of industrial wastewater in smart cities: a sensitive solution, Sustain. Energy Technol. Assessments 55 (2023), 102967.
[40] U. Srimathi, V. Nagarajan, R. Chandiramouli, Investigation on graphdiyne nanosheet in adsorption of sorafenib and regorafenib drugs: a DFT approach, J. Mol. Liq. 277 (2019) 776–785.
[41] M. Shahabi, H. Raissi, Screening of the structural, topological, and electronic properties of the functionalized Graphene nanosheets as potential Tegafur anticancer drug carriers using DFT method, J. Biomol. Struct. Dyn. 36 (2018) 2517–2529.
[42] M. Shahabi, H. Raissi, Investigation of the solvent effect, molecular structure, electronic properties and adsorption mechanism of Tegafur anticancer drug on Graphene nanosheet surface as drug delivery system by molecular dynamics simulation and density functional approach, J. Inclusion Phenom. Macrocycl. Chem. 88 (2017) 159–169.
[43] M. Vatanparast, Z. Shariatinia, Hexagonal boron nitride nanosheet as novel drug delivery system for anticancer drugs: insights from DFT calculations and molecular dynamics simulations, J. Mol. Graph. Model. 89 (2019) 50–59.
[44] A. Tariq, S. Nazir, A.W. Arshad, F. Nawaz, K. Ayub, J. Iqbal, DFT study of the therapeutic potential of phosphorene as a new drug-delivery system to treat cancer, RSC Adv. 9 (2019) 24325–24332.
[45] C.R. Dean, A.F. Young, I. Meric, C. Lee, L. Wang, S. Sorgenfrei, K. Watanabe, T. Taniguchi, P. Kim, K.L. Shepard, Boron nitride substrates for high-quality graphene electronics, Nat. Nanotechnol. 5 (2010) 722–726.
[46] A. Pakdel, C. Zhi, Y. Bando, T. Nakayama, D. Golberg, Boron nitride nanosheet coatings with controllable water repellency, ACS Nano 5 (2011) 6507–6515.
[47] J. Yu, L. Qin, Y. Hao, S. Kuang, X. Bai, Y.-M. Chong, W. Zhang, E. Wang, Vertically aligned boron nitride nanosheets: chemical vapor synthesis, ultraviolet light emission, and superhydrophobicity, ACS Nano 4 (2010) 414–422.
[48] F. Hui, C. Pan, Y. Shi, Y. Ji, E. Grustan-Gutierrez, M. Lanza, On the use of two dimensional hexagonal boron nitride as dielectric, Microelectron. Eng. 163 (2016) 119–133.
[49] Y. Zhang, Z. Xia, Q. Li, G. Gui, G. Zhao, S. Luo, M. Yang, L. Lin, Copper/hexagonal boron nitride nanosheet composite as an electrochemical sensor for nitrite determination, Int. J. Electrochem. Sci. 13 (2018) 5995–6004.
[50] T.S. Ashton, A.L. Moore, Foam-like hierarchical hexagonal boron nitride as a non-traditional thermal conductivity enhancer for polymer-based composite materials, Int. J. Heat Mass Tran. 115 (2017) 273–281.
[51] P. Ahmad, M.U. Khandaker, N. Muhammad, F. Rehman, G. Khan, M.A. Rehman, S.M. Ahmed, M. Gulzar, A. Numan, A.S. Khan, Synthesis of multilayered hexagonal boron nitride microcrystals as a potential hydrogen storage element, Ceram. Int. 43 (2017) 7358–7361.
[52] S. Singh, J. Singh, S. Goyal, S.S. Sehra, F. Ali, M.A. Alkhafaji, R. Singh, A novel framework to avoid traffic congestion and air pollution for sustainable development of smart cities, Sustain. Energy Technol. Assessments 56 (2023), 103125.
[53] Y. Fujii, M. Maruyama, N.T. Cuong, S. Okada, Pentadiamond: a hard carbon allotrope of a pentagonal network of sp 2 and sp 3 C Atoms, Phys. Rev. Lett. 125 (2020), 016001.
[54] S. Iijima, T. Ichihashi, Y. Ando, Pentagons, heptagons and negative curvature in graphite microtubule growth, Nature 356 (1992) 776–778.

[55] A. Loiseau, F. Willaime, N. Demoncy, G. Hug, H. Pascard, Boron nitride nanotubes with reduced numbers of layers synthesized by arc discharge, Phys. Rev. Lett. 76 (1996) 4737–4740.
[56] A.M. Heitzer, J. Longoria, V. Okhomina, W.C. Wang, D. Raches, B. Potter, L.M. Jacola, J. Porter, J.E. Schreiber, A.A. King, Hydroxyurea treatment and neurocognitive functioning in sickle cell disease from school age to young adulthood, Br. J. Haematol. 195 (2021) 256–266.
[57] S. Kapor, V. Čokić, J.F. Santibanez, Mechanisms of hydroxyurea-induced cellular senescence: an oxidative stress connection? Oxid. Med. Cell. Longev. 2021 (2021) 1–16.
[58] C.A. Bulte, K.M. Hoegler, Ö. Kutlu, A. Khachemoune, Hydroxyurea: a reappraisal of its cutaneous side effects and their management, Int. J. Dermatol. 60 (2021) 810–817.
[59] J. Morris, K. Ergun, B. Khaleghi, M. Imani, B. Aksanli, T. Rosing, Hydrea: towards more robust and efficient machine learning systems with hyperdimensional computing, in: 2021 Design, Automation & Test in Europe Conference & Exhibition (DATE), IEEE, 2021, pp. 723–728.
[60] X. Xue, H. Liu, S. Wang, Y. Hu, B. Huang, M. Li, J. Gao, X. Wang, J. Su, Neutrophil-erythrocyte hybrid membrane-coated hollow copper sulfide nanoparticles for targeted and photothermal/anti-inflammatory therapy of osteoarthritis, Compos. B Eng. 237 (2022), 109855.
[61] M. Safari Kakroudi, S. Rimaz, Z. Atrkar Roshan, M. Mobayen, The frequency of bacterial colonization in burn wounds and antibiogram pattern in patients hospitalized in the ICU of velayat burn and reconstructive surgery center in rasht city, Int. J. Sci. Res. Dental Med. Sci. 1 (2019) 72–79.
[62] Y. Liu, Z. Luo, J.Z. Zhang, F. Xia, DFT calculations on the mechanism of transition-metal-catalyzed reaction of diazo compounds with phenols: O–H insertion versus C–H insertion, J. Phys. Chem. 120 (2016) 6485–6492.
[63] A.K. Jissy, A. Datta, Effect of external electric field on H-bonding and π-stacking interactions in guanine aggregates, ChemPhysChem 13 (2012) 4163–4172.
[64] E.D. Glendening, C.R. Landis, F. Weinhold, NBO 6.0: natural bond orbital analysis program, J. Comput. Chem. 34 (2013) 1429–1437.
[65] S. Lakshminarayanan, V. Jeyasingh, K. Murugesan, N. Selvapalam, G. Dass, Molecular electrostatic potential (MEP) surface analysis of chemo sensors: an extra supporting hand for strength, selectivity & non-traditional interactions, J. Photochem. Photobiol., A 6 (2021), 100022.
[66] K. Harismah, M.M.R. Nayini, S. Montazeri, S. Ariaei, M. Nouraliei, DFT investigation of SiO 2 nanotube for adsorption of methyl-and propyl-paraben, Main Group Chem. 20 (2021) 355–363.
[67] J.B. Frank, T.R. Kosten, E.L. Giller Jr., E. Dan, A randomized clinical trial of phenelzine and imipramine for posttraumatic stress disorder, Am. J. Psychiatr. 145 (1988) 1289–1291.
[68] N. Zainuddin, I. Ahmad, M.H. Zulfakar, H. Kargarzadeh, S. Ramli, Cetyltrimethylammonium bromide-nanocrystalline cellulose (CTAB-NCC) based microemulsions for enhancement of topical delivery of curcumin, Carbohydr. Polym. 254 (2021), 117401.